Published in final edited form as:
Cancer Prev Res (Phila). 2010 May ; 3(5): 630–639. doi:10.1158/1940-6207.CAPR-10-0003.

Deficiency in the 15 kDa Selenoprotein Inhibits Tumorigenicity and Metastasis of Colon Cancer Cells

Robert Irons[1,2,4,6], **Petra A. Tsuji**[1,2,3,6], **Bradley A. Carlson**[2], **Ping Ouyang**[1,2], **Min-Hyuk Yoo**[2], **Xue-Ming Xu**[2], **Dolph L. Hatfield**[2], **Vadim N. Gladyshev**[5], and **Cindy D. Davis**[1,8]

[1]Nutritional Science Research Group, National Cancer Institute, Rockville, MD 20892

[2]Molecular Biology of Selenium Section, Laboratory of Cancer Prevention, National Cancer Institute, Bethesda, MD 20892

[3]Cancer Prevention Fellowship Program, National Cancer Institute, Rockville, MD 20892

[4]V.E. Irons, Inc., Kansas City, MO 64106

[5]Brigham and Women's Hospital, Harvard Medical School, Boston, MA 02115

Abstract

Selenium has cancer preventive activity that is mediated, in part, through selenoproteins. The role of the 15 kDa selenoprotein (Sep15) in colon cancer was assessed by preparing and using mouse colon CT26 cells stably transfected with shRNA constructs targeting Sep15. Metabolic ^{75}Se-labeling, Northern and Western blot analyses revealed that more than 90% of Sep15 was down-regulated. Growth of the resulting Sep15-deficient CT26 cells was reduced ($p<0.01$) and cells formed significantly ($p<0.001$) fewer colonies in soft agar compared to control CT26 cells. Whereas most (14/15) BALB/c mice injected with control cells developed tumors, few (3/30) mice injected with Sep15-deficient cells developed tumors ($p<0.0001$). The ability to form pulmonary metastases had similar results. Mice injected with the plasmid-transfected control cells had >250 lung metastases/ mouse; however, mice injected with cells with down-regulation of Sep15 only had 7.8± 5.4 metastases. To investigate molecular targets affected by Sep15 status, gene expression patterns between control and knockdown CT26 cells were compared. Ingenuity Pathways Analysis was used to analyze the 1045 genes that were significantly ($p<0.001$) affected by Sep15 deficiency. The highest scored biological functions were cancer and cellular growth and proliferation. Consistent with these observations, subsequent analyses revealed a G2/M cell cycle arrest in cells with targeted down-regulation of Sep15. In contrast to CT26 cells, Sep15 -targeted down-regulation in Lewis Lung Carcinoma (LLC1) cells did not affect anchorage-dependent or –independent cell growth. These data suggest tissue specificity in the cancer protective effects of Sep15 down-regulation, which are mediated, at least in part, by influencing the cell cycle.

Keywords

15 kDa selenoprotein; colon cancer; CT26 cells; LLC1 cells; shRNA technology

[8]Corresponding author and to whom reprint requests should be addressed: Cindy D. Davis, Ph.D., Nutritional Science Research Group, Division of Cancer Prevention, National Cancer Institute, 6130 Executive Boulevard, Suite 3159, Rockville, MD 20892-7328, tel: 301-594-9692, fax: 301-480-3925.

[6]Co-First Authors

[9]The authors have no conflicts of interest

Introduction

Colorectal cancer is the third most commonly diagnosed cancer in Americans and is the second leading cause of cancer mortality. Epidemiologic, clinical and preclinical studies provide evidence that the essential trace mineral selenium may protect against colon cancer (1). Supplemental selenium has been found to reduce the incidence and mortality of colon cancer in humans (2). This is consistent with animal studies showing protective effects of selenium against carcinogen-induced aberrant crypt formation and colon tumor development (3,4). Some of these biological changes are likely attributable to selenium's role as a constituent of specific proteins. Moreover, recent studies have implicated both selenoproteins and low molecular weight selenocompounds as playing important roles in the cancer protective effects of selenium in the colon (5).

The 15 kDa selenoprotein gene (*Sep15*) is one of 24 known selenoprotein genes in rodents (6). The gene product, Sep15, exhibits redox activity (7) and belongs to the class of thiol-disulfide oxidoreductase-like selenoproteins (8). Sep15 is structurally similar to the thioredoxin superfamily (8). Although decreased expression of Sep15 has been observed in liver, prostate and lung cancer, the expression of Sep15 in colon cancer is less clear (7). Analysis of the National Cancer Institute's Developmental Therapeutics Program database (http://dtp.nci.nih.gov/mtweb/targetdata), which screens 60 tumor cell lines for molecular targets, demonstrated increased Sep15 expression in colon cancer cell lines compared to other cancers as well as compared to other selenoproteins. Moreover, in humans, Sep15 is located on chromosome 1p31, a locus commonly mutated in human cancer (9).

The purpose of this study was to assess the role of Sep15 in colon cancer. RNA interference technology was used to specifically down-regulate Sep15 expression in a mouse colon cancer cell line, CT26. These cells were derived from an N-nitroso-N-methylurethane-induced BALB/c undifferentiated colon carcinoma (10). Herein, we report that targeted down-regulation of Sep15 in CT26 cells decreased growth under anchorage-dependent and -independent conditions, inhibited tumor formation *in vivo* and reduced lung metastasis. In contrast, targeted down-regulation of Sep15 in mouse Lewis Lung Carcinoma (LLC1) cells did not affect the ability of the cells to grow in culture or in soft-agar. These studies reveal a complex role of Sep15 in cancer development.

Materials and Methods

The murine CT26 colon cancer and LLC1 lung cancer cells were purchased from American Type Culture Collection (ATCC, Manassas, VA). ^{75}Se (specific activity ~1,000 Ci/mmol) was obtained from the Research Reactor Facility at the University of Missouri (Columbia, MO) and [α-^{32}P] dCTP (specific activity ~ 6,000 Ci/mmol) from Perkin Elmer (Waltham, MA). pSliencer 2.0 U6 Hygro vector was purchased from Ambion (Foster City, CA) and Hybond N^+ nylon membranes from GE Healthcare (Piscataway, NJ). RPMI 1640 medium, fetal bovine serum, hygromycin B, NuPage® 4-12% polyacrylamide gels, LDS sample buffer, See-Blue Plus2 protein markers, polyvinylidene difluoride membranes, Lipofectamine 2000 and TRIzol® reagent were purchased from Invitrogen (Carlsbad, CA) and 5,5′-dithio-bis(2-nitrobenzoic acid) and aurothioglucose (ATG) from Sigma-Aldrich (St. Louis, MO).

Antibodies against Sep15 were generated in our laboratories using recombinant Sep15 as antigen. Horseradish peroxidase-conjugated secondary antibody was obtained from Santa Cruz Biotechnology (Santa Cruz, CA), SuperSignal West Dura substrate from Pierce (Rockford, IL). iScript™ cDNA synthesis Kit and SYBR green supermix were purchased from Bio-Rad Laboratories (Philadelphia, PA). Primers for real-time PCR were purchased from Sigma-Genosys (St. Louis, MO), Noble agar from Becton, Dickinson and Company (BD, Franklin

Lakes, NJ), and Black India Ink from Winsor & Newton (Harrow, Middlesex, England). Other reagents used were commercially available and were of the highest quality available.

Targeted down-regulation of Sep15

The pU6-m3 vector used for generating shRNA targets was constructed as described elsewhere (11,12). To down-regulate *Sep15* expression, two separate 19-nt sequences, 5′-gcaccacagtccataatat-3′ (shSep15-1) and 5′-acagaagagttccatttaa-3′ (shSep15-2) were chosen from the mouse *Sep15* cDNA, which were unique to this gene. These sequences were annealed and inserted into the *BamH*I-*Hind*III cloning sites in pU6-m3 as previously described (11).

Culture of mammalian cells and cell growth assays

CT26 cells were cultured in growth medium (RPMI 1640 medium supplemented with 10% fetal bovine serum, 1% sodium pyruvate, and 500 μg/ml hygromycin B) in a humidified atmosphere with 5% CO_2 at 37°C. LLC1 cells were cultured in Dulbecco's Modified Eagle Medium (DMEM, supplemented with 10% heat-inactivated fetal bovine serum and 500 μg/ml hygromycin B). Both malignant cell lines were stably transfected with shSep15-1, shSep15-2 or pU6-m3 constructs using Lipofectamine 2000 by selecting cells in the presence of 500 μg/ml of hygromycin B.

Cell growth was monitored by seeding cells in 6-well plates at 1×10^5 cells per well in complete growth medium and counting cells for four days. For the cell growth assays under conditions of varying selenium concentrations, CT26 cells were seeded in 6-well plates at 2×10^5 cells per well in complete culture medium, wherein the cells attached to the bottom of the wells. After 24 hours, growth medium was discarded, cells were washed twice with PBS, and subsequently fed with 2 ml of serum-free medium (RPMI medium supplemented with 1% sodium pyruvate, 500μg/ml hygromycin B, 5μg/ml insulin and 5μg/ml of transferrin) supplemented with none, 0.1 μM, 0.5 μM or 1.0 μM selenium in the form of sodium selenite. The total number of cells was counted daily for four days in serum-free medium.

Real Time RT-PCR analysis

Total RNA was extracted from cells using TRIzol® Reagent. cDNA was synthesized using iScript™ with 2 μg of total RNA. For real-time qPCR, 1.5 μl of cDNA was used in 20 μl reactions using the DNA Engine Opticon® 2 Real-Time PCR Detection System (MJ-Research/BioRad Laboratories, Hercules, CA). The primers used for real-time PCR are shown in Supplementary Table 1. The mRNA levels of selenoproteins were calculated relative to the expression of *β*-glucuronidase (*Gusb*) and/or GAPDH was utilized as the internal control.

Western blot analysis

Protein extracted from the three CT26 cell lines was electrophoresed on a NuPage® 4-12% polyacrylamide gel followed by transferring to a polyvinylidene difluoride membrane. The membrane was incubated with a rabbit polyclonal Sep15 antibody overnight. Horseradish peroxidase-conjugated anti-rabbit secondary antibody (1:5,000) was applied, and the membrane was incubated in chemiluminescent substrate and exposed to X-ray film.

^{75}Se labeling of cells

CT26 cells were seeded in a six-well plate (5×10^5 cells/well), incubated for 18 h, and then labeled with 50 μCi/well of ^{75}Se for 24 h before harvesting. Cells were suspended in 1× NuPage® LDS sample buffer, sonicated and 20 μg protein were electrophoresed on a NuPage® 4-12% polyacrylamide gel. The gel was stained with Coomassie Blue, dried, and exposed to a PhosphorImager screen (Molecular Dynamics, GE Healthcare, Piscataway, NJ).

Northern blot analysis

Total RNA was isolated using TRIzol® reagent. An equal amount of RNA (15 μg) from each cell line was loaded onto gels and transferred to a nylon membrane. The membrane was hybridized with a ^{32}P-labeled Sep15 cDNA probe prepared as described previously (13). The membrane was stripped and re-probed with a ^{32}P-labeled GAPDH cDNA probe.

Enzyme activities

Glutathione peroxidase (GPx) activity was measured by the coupled assay procedure (14), which uses hydrogen peroxide as substrate. This assay measures both GPx1 and GPx2 activity. Data are expressed as units/mg protein. TR activity was determined spectrophotometrically by the method of Holmgren and Bjornstedt (15) as modified by Hill *et al.* (16) and Hintze *et al.* (17). Activity was determined by subtracting the time-dependent increase in absorbance at 412 nm in the presence of the thioredoxin reductase activity inhibitor, aurothioglucose, from total activity. A unit of activity was defined as 1.0 μmol 5-thio-2-nitrobenzoic acid formed /min/mg protein. Protein concentrations were measured using the BCA reagent.

Soft agar assay

Anchorage-independent growth was assayed as described previously (11) with the exception that herein a total of 3,000 cells of each stably transfected CT26 cell line were suspended in 3 ml of 0.35% agar in complete RPMI medium and spread onto 60 mm Petri dishes masked with a basal layer of 3 ml 0.7% agar in medium. For LLC1 cells, a total of 1,000 cells/3 ml was applied. Cells were incubated at 37°C for 20 days (12 days for LLC1 cells), and complete growth medium was applied to the dishes every 3 to 5 days. The colonies were visualized by staining with ρ-iodonitrotetrazolium violet overnight, scanned and counted.

Cell cycle analysis

CT26 cells were grown in complete medium to 40% confluency, washed twice with PBS, and maintained in serum-free medium for 48 h to induce G_0/G_1 cell cycle synchronization. Cells were then washed twice with PBS and growth stimulated with complete growth medium for 24 h. Cells were then twice washed with PBS, trypsinized and suspended in PBS ($1\text{-}2 \times 10^7$ cells/ml) on ice. Ice-cold 70% ethanol was added gradually and cells were fixed overnight. Cells were centrifuged and resuspended in RNAse (100 units) and incubated at 37°C for 20 min. The suspension was stained with propidium iodide in the dark at 4°C over night, filtered through a 50 micron mesh, and acquired with a BD FACScalibur™ (Franklin Lakes, NJ). The number of cells in each phase of the cell cycle was analyzed by ModFit LT v.3.0 (Verity, Topsham, ME).

Microarray analysis

mRNA was isolated from plasmid-transfected control and shSep15 knockdown CT26 cells (n=3 for each). Microarray analysis was performed on Affymetrix Mouse 430_2 gene chips. Three arrays were analyzed from different mRNA samples for each construct. The false discovery rate was set at <0.01. Controls and cells with targeted down-regulation of Sep15 were compared by ANOVA. The ANOVA list can be calculated from our data accessible through GEO Series accession number GSE20390 (http://www.ncbi.nlm.nih.gov/geo/query/acc.cgi?acc=GSE20390) Those genes significantly different from the control cells at the $p<0.001$ level were subjected to functional gene analysis using the DAVID functional annotation tool (18,19) and the Ingenuity Pathway Analysis (IPA v. 7.5, Redwood City, CA). IPA groups significantly linked genes according to the biological processes in which they function. The program displays their significance values, the interacting genes, and direct or indirect association patterns. The networks created were ranked depending on the number of significantly expressed genes they contain.

Animal studies

All animal protocols and animal care was in accordance with the National Institutes of Health's guidelines for care and use of laboratory animals under the direction of Dr. John Dennis (NCI, NIH, Bethesda, MD). Male BALB/c mice were obtained from Jackson Labs (Bar Harbor, ME) and maintained in a temperature- and humidity-controlled animal facility with a 12-h light/dark cycle. Animals were given free access to water, and were monitored closely for any clinical signs of poor health throughout the study.

Male three week-old BALB/c mice were maintained on a selenium-deficient Torula yeast based diet that was supplemented with 0 μg, 0.1 μg or 2.0 μg selenium/g diet as sodium selenite (Teklad, Harlan Laboratories, Madison, WI) for three weeks prior to being injected subcutaneously with 1×10^6 CT26 cells (n=5 for plasmid-transfected controls, shSep15-1 or shSep15-2 cells on each diet) in 200 μl PBS. Animals were sacrificed three weeks post-injection. Tumors, if present, were excised, measured, weighed and snap frozen and stored at -80°C for future analyses.

For the lung metastasis study, six-week old male BALB/c mice were maintained on mouse chow for three weeks prior to intravenous injection into the tail vein with plasmid-transfected control or shSep15 CT26 cells (5×10^5 cells/mouse) in 200 μl PBS. Animals were sacrificed and lungs were examined 12 days after i.v. injection. Three ml of 15% India Ink/PBS solution were injected into the lungs through the trachea. Lung tissues were excised and “bleached” by Fekete's solution (60% ethanol, 3.2% formaldehyde, and 0.75 M acetic acid). Lobes of the lungs were separated and the pulmonary metastatic lesions formed on the surface of each lung were counted under a dissecting microscope. Lungs with more than 250 metastatic lesions were assigned a value of 250, because of the inherent difficulty to reliably count numbers over 250 lesions per lung. Three independent experiments were conducted.

Statistical analyses

Data are presented as means ± S.E. Data were analyzed by ANOVA followed by Tukey's Multiple Comparison post-hoc test using GraphPad Prism (v.4) (LaJolla, CA). The level of significance was set at $p< 0.05$.

Results

Gene expression for all 24 mouse selenoprotein genes was determined in CT26 cells by real time PCR analysis (Figure 1). Seventeen selenoprotein mRNAs were detected. Sep15 mRNA had the highest mRNA expression level, and other highly expressed genes included GPx4 and GPx1. To prepare cells characterized by Sep15 deficiency, CT26 cells were stably transfected with shSep15-1, shSep15-2 or the corresponding pU6-m3 control constructs. Each of the stably transfected cell lines was initially labeled with ^{75}Se to examine the levels of Sep15 and other selenoproteins, and the relative intensities of ^{75}Se-labeled proteins were determined using a PhosphorImager (Figure 2A). Both cells with targeted down-regulation of Sep15 significantly reduced the levels of ^{75}Se-labeled Sep15. Northern (Figure 2B) and western (Figure 2C) blot analyses also demonstrated that Sep15 mRNA and protein expression, respectively, were efficiently (>90%) decreased by both shRNA vectors. In contrast, ^{75}Se labeling of other selenoproteins, such as TR1, GPx1 and GPx4, did not change (Figure 2A) nor were their catalytic activities (Figures 2D and 2E) affected by the shSep15 constructs.

The growth rate of the shSep15-1 and shSep15-2 mouse colon carcinoma CT26 cells was significantly reduced ($p<0.01$) beginning at three days and was 40-50% fewer cells at four days compared with the pU6-m3-transfected control cells (Figure 3A). Changing the selenium concentration in the growth medium from 0 to 1 μM did not significantly affect cell growth of

the cells with Sep15 targeted-downregulation compared to the control cells (Supplementary Figure 1).

To extend these findings to other cell lines, stably transfected mouse LLC1 cells with the same constructs for Sep15 targeted-downregulation as the CT26 cells were developed. A greater than 90% knockdown efficiency was achieved as verified by real-time RT-PCR (Supplementary Figure 2A). While the basal expression of Sep15 is higher in CT26 than in LLC1 cells (27.65 versus 5.31 units relative to GusB, respectively), this level of expression is still almost 10-fold higher than in the CT26 cells with targeted downregulation of Sep15 (0.59 units relative to GusB). However, in contrast to the growth of CT26 cells, the growth rate of shSep15-1 and shSep15-2 transfected LLC1 cells was not altered compared to that of the pU6-m3 transfected LLC1 control cells (Supplementary Figure 2B).

Another characteristic of many cancer cells is their ability to grow unanchored in soft agar; whereas many normal cells do not grow under such conditions. After 20 days growth in soft agar, the colonies of cells transfected with either the pU6-m3 control or the Sep15 targeted-downregulation constructs were stained, scanned and quantitated (Figure 3B). Compared to the pU6-m3 transfected control cells, the shSep15-1 and shSep15-2 transfected CT26 cells had formed significantly ($p<0.01$) fewer colonies (2470 ± 140 versus 668 ± 33 and 512 ±83 colonies, respectively) (Figure 3C). In contrast to the findings with CT26 colon carcinoma cells, Sep15 targeted down-regulation in LLC1 lung carcinoma cells did not affect the ability of cells to grow in soft agar. The shSep15-1 and shSep15-2 transfected cells formed 521±19 and 505±10 colonies, respectively, whereas the control LLC1 cells had 529±12 colonies (Figure 3D). These data suggest that Sep15 targeted-downregulation in LLC1 cells does not influence anchorage-dependent or –independent cell growth.

The ability of CT26 cells with targeted down-regulation and control cells to form tumors was measured by injecting them subcutaneously into mice of the same genetic background. Control cells retained their tumorigenic ability and resulted in subcutaneous tumors in injected mice (Figure 4A). Most (14/15) of the animals injected with control cells developed tumors; dietary selenium appeared to dose-dependently decrease tumor weight in animals injected with control cells. In contrast, only one (1/15) of the animals injected with shSep15-2 CT26 cells developed a tumor ($p<0.0001$). Moreover, since the constructs were retained in stably transfected cells with hygromycin B, and the injected mice could not be treated with this antiobiotic, it was possible that the tumor which grew in the mouse injected with shSep15-2-transfected cells was a result of loss of the shSep15 targeting vector. Indeed, RT-PCR analysis demonstrated that tumors from both the control and cells with targeted down-regulation expressed appreciable Sep15 mRNA (Figure 4B). However, because only one tumor was formed when the shSep15-2 knockdown cells were utilized, another 15 mice with the shSep 15-1 knockdown cells were examined. Similar to the results with the shSep 15-2 knockdown cells, very few animals injected with shSep 15-1 were able to develop tumors (2/15) and the tumors that were formed had no difference in Sep15 expression compared to tumors formed in mice injected with control cells (0.13±0.02 versus 0.18±0.07 units relative to GAPDH, $p>0.05$). These data suggest that residual tumor growth in mice injected with the shSep15-transfected cells is dependent on Sep15 expression.

In addition to inhibiting tumor growth, targeted down-regulation of Sep15 also inhibited the ability to form pulmonary metastatic lesions upon i.v. administration of cells (Figure 4C,D). Mice injected with the plasmid-transfected control cells had >250 lung metastasis/mouse; however, mice injected with the shSep15 cells only had 8 ± 5 metastases.

Microarray analysis was conducted to elucidate possible mechanism(s) whereby Sep15 deficiency inhibited CT26 cancer cell growth, ability to grow in soft agar, tumorigenicity and

metastasis. Comparison of gene expression changes between cells with targeted down-regulation of Sep15 and pU6-m3 control cells revealed 1045 genes out of a total number of 45,101 genes and their variants examined that were statistically ($p<0.001$ level) different. The most significantly up-regulated and down-regulated genes and their protein products are listed in Table 1. Further examination with the DAVID functional annotation gene ontology tool demonstrated that genes in several areas were affected, including cell cycle (G2/M phase arrest), protein localization and metabolism. Analysis with IPA demonstrated that the top 5 associated networks were related to cancer, cell cycle or cellular function and maintenance. These included: “Cellular assembly and organization/cellular function and maintenance/cell morphology”, “DNA replication/recombination and repair/cell cycle/cancer”, and “Cancer/cell-to-cell signaling and interaction/cellular function and maintenance” (Figure 5). Genes depicted in red have up--regulated and genes in green have downregulated expression in shSep15 knockown cells compared to control cells. A list of the genes which had the most significantly increased or decreased expression in the Sep15 targeted down-regulation compared to the control cells are shown in Table 1. The gene whose expression changed the most was *Ccnb1ip1*. When the significantly altered genes were analyzed for biological function, the primary disease being altered was cancer (302 significantly modified genes) and the primary molecular and cellular function was cellular growth and proliferation (246 significantly modified genes) and cell death (216 significantly modified genes).

Quantitative RT-PCR was utilized to validate the results of the microarray analysis. Comparison of data from qRT-PCR and microarray demonstrated a similar magnitude and direction of the response in the mRNA expression of CCNB1IP1 (10.03 and 13.52 fold increased expression via qRT-PCR and microarray, respectively), cyclin B1 (4.8 and 2.4 fold increased expression via qRT-PCR and microarray, respectively) in cells with targeted down-regulation compared to control cells. Similar results were also observed for several selenoprotein genes (Sep15, GPx1, GPx4, SelM and SelK). For example, Sep15 was inhibited 98.2% and 95.3% when analyzed by qRT-PCR and microarray, respectively. None of the other selenoproteins demonstrated significant changes in gene expression.

FACS analysis was then employed to validate the G2/M cell arrest suggested by the microarray analysis. The shSep15 cells had a higher percentage of cells in G2/M (21.2±1.1 versus 13.3 ±0.9%) and G0/G1 (57.3±1.4 versus 51.0±1.1%) and a smaller percentage of cells in S phase (21.6±0.5 versus 35.7±0.5%, mean±SEM, n=8) compared to the control cells.

Discussion

While recent data have demonstrated that both selenoproteins and low molecular weight selenocompounds may mediate the cancer-protective effects of selenium, few studies have addressed the role of specific selenoproteins (5). The current studies help with this void by evaluated selenoprotein expression in mouse CT26 colon cancer cells. Because Sep15 was the highest expressed selenoprotein mRNA in these cells and little is known about its biological effects, cells with targeted down-regulation of Sep15 were then generated by stable transfection with two different Sep15-specific sequences and compared with plasmid transfected control cells. Suprisingly, the cells with targeted down-regulation of Sep15 exhibited decreased colony formation in soft agar (Figure 3), as well as lower tumor formation and decreased ability to form lung metastasis (Figure 4) compared to the control cells. Since the Sep15 deficient cell lines and the corresponding CT26 parental cells were transfected with identical vectors (described in detail elsewhere (11,22, 29, 30)) except for the shRNAs in the two Sep15 down-regulated cells, these changes are most certainly due to the loss of this selenoprotein. These results suggest that targeted down-regulation of Sep15 is protective against tumorigenesis in these colon cancer cells or that Sep 15 might be important for tumorigenesis.

In contrast to these findings, previous observations have suggested that Sep15 expression is decreased in mouse liver tumors and mouse prostate adenocarcinoma cells compared to the high levels of this protein expressed by normal mouse liver and prostate (7). Similarly, Sep15 was down-regulated in approximately 60% of human malignant mesothelioma cell lines and tumors (20). However, it should be noted that there was significant variability among the cell lines and four of the 23 mesothelioma cells lines had over-expression of Sep15. When one of the cell lines, Meso 6, was transiently transfected with siRNA against *Sep15*, the cells exhibited increased cell proliferation following exposure to pharmacological concentrations of selenium (1-25 μM) compared to Meso 6 cells that possessed the wild-type *Sep15* (20). While selenium supplementation did not influence the growth of cells with targeted down-regulation of Sep15 in the current study, the cells were grown under conditions more close to the physiological state (0-1 μM Se). Moreover, differences could also be a result of transient versus stable transfection. Regardless, these data suggest that mesothelioma cells respond differently to targeted down-regulation of Sep15 than CT26 colon cancer cells, suggesting that there might be tissue specificity in the response.

Apostolou et al. (20) observed that mesothelioma cells with the 1125A variant within the 3′-UTR of Sep15 were less responsive to the growth inhibitory and apoptotic effects of selenium as selenocysteine than mesothelioma cells expressing the wild-type protein. It has been shown that the SECIS element with the A at position 1125 is more efficient in stimulating selenocysteine insertion than the SECIS element containing G at position 1125. Jablonska et al. (21) evaluated whether this single nucleotide polymorphism in Sep15 in combination with selenium status is associated with lung cancer risk. They observed that interactions between selenium status and this polymorphism in non-small cell lung cancer patients are complex and depend on the selenium status of the individual (20). Unfortunately, the expression of Sep15 in the lung tumors was not measured. However, because of the previously published data suggesting that Sep15 expression might be down-regulated in certain lung cancers, as well as mouse liver and prostate tumors, we wanted to determine whether the effects might be specific to colon cancer. In contrast to observations with CT26 cells, lung carcinoma LLC1 cells transfected with the shSep15 constructs did not change growth characteristics in culture or alter their ability to grow colonies in soft agar (Figure 3). These observations further indicate that there is tissue specificity in the response of mouse tumor cells to Sep15 status. Whereas targeted down-rgulation of Sep15 is protective against tumorigenesis in colon CT26 cells, it does not affect tumorigenesis in lung LLC cells. We are currently investigating whether these observations occur in human colon cancer cell lines and the mechanism(s) accounting for tissue specificity.

While there is evidence to suggest that supplemental selenium may reduce the incidence and mortality of colon cancer in humans (2), this effect appears to be mediated by both low molecular weight selenocompounds and selenoproteins. Moreover, not all selenoproteins may inhibit tumorigenesis. The observation that targeted down-regulation of a selenoprotein may be protective against tumorigenesis is not unique for Sep15. Previous data have shown that targeted down-regulation of TR1 reverses the tumor phenotype of LLC1 cells (11) and inhibits self-sufficient growth of a mouse cell line driven by oncogenic *k-ras* (DT) cells (22). TR1 is a central component in redox-regulated pathways and its main function is to keep thioredoxin in the reduced state (23). Thioredoxin can then donate electrons to disulfides in both cytosolic and nuclear proteins and thus maintain the cysteine residues in these proteins in the reduced state. Similar to TR1, Sep15 belongs to the thiol-disulfide oxidoreductase class of selenoproteins (7,8). Sep15 is characterized by a thioredoxin fold and has been shown to take part in the process of disulfide bond formation. While the physiological function and catalytic mechanism of Sep15 remain poorly understood, it has been hypothesized that Sep15 is involved in either rearrangement of disulfide bonds (isomerase function) or reduction of incorrectly formed disulfide bonds (reductase function) in misfolded glycoproteins bound to UDP-

glucose: glycoprotein glucosyltransferase (UGGT) (24). While it is intriguing that targeted down-regulation of either TR1 or Sep15 can be protective against tumorigenesis, it is not known how these two proteins interact. Future studies are needed to investigate the interrelationship of Sep15 and TR in tumorigenesis.

Development of cancer requires multiple changes in the regulation of cell physiology. Hannahan and Weinberg (25) defined criteria that are necessary for the formation of an aggressive tumor: a cell must autonomously provide growth signals, become insensitive to growth-inhibitory signals, inactivate proapoptoic pathways, acquire a limitless replicative potential, promote angiogenesis and become able to invade tissues and metastasize. Some tumor suppressor genes and oncogenes function specifically in these phenotypes. We utilized microarray technology to determine the most important genes whose expression was modified by targeted down-regulation of Sep15. While many of the changes in gene expression observed in the cells with targeted down-regulation of Sep15 might be a general response to growth inhibition, microarray technology allowed us to determine the specific molecular target(s) for this growth inhibition. Interestingly, *Ccnb1ip1* was the most significantly upregulated gene in Sep15 knockdown compared to control cells (>13.5 fold increase, Table 1) which was validated by qRT-PCR. This gene encodes cyclin B1 interacting protein 1 (CCNB1IP1) which functions as a RING-finger family ubiquitin ligase (26). Protein ubiquitination is critical for many cellular processes, through its ability to regulate protein degradation and various signaling mechanisms. CCNB1IP1 functions by modulating progression of the cell cycle through G2/M by interacting with cyclin B and promoting its degradation (26). Alterations in the cell cycle in cells with targeted down-regulation of Sep 15 compared to control cells were validated by FACS analysis. CCNB1IP1 also influences the processes of cell migration and metastasis. Interestingly, human osteosarcoma cells and human breast cancer cells depleted in CCNB1IP1 both migrate more rapidly and invade more effectively than control cells (27). Similarly, down-regulation of CCNB1IP1 has been associated with aggressive breast cancer and non-small cell lung cancer and predicted poor prognosis (28). Consistent with these observations, an increased expression of CCNB1IP1 was observed in the cells with targeted down-regulation of Sep15, which correlated with a decreased ability to grow and metastasize.

In conclusion, the current investigations conclusively demonstrate that Sep15 shRNA-transfection of mouse colon carcinoma CT26 cells (>90% reduction of Sep15 mRNA and protein levels) inhibited anchorage-dependent and -independent cell growth as well as tumor growth and lung metastasis. This response is mediated, at least in part, by increased expression of CCNB1IP1 and subsequent G2/M cell cycle arrest in mouse colon cancer cells. Furthermore, tissue specificity in the ability of Sep 15 to influence cellular proliferation was evident.

Acknowledgments

The authors would like to thank Dr. John Milner, Division of Cancer Prevention, National Cancer Institute for his helpful support, discussion and review of the manuscript. We would also like to acknowledge the assistance of the following individuals from the Center for Cancer Research, National Cancer Institute: Dr. Salvador Naranjo-Suarez with the IPA analysis, Dr. Barbara Taylor with FACS analysis and Dr. Paul Goldsmith with the catalytic assays.

Funded by NCI Intramural support, the Cancer Prevention Fellowship Program and the Division of Cancer Prevention and NIH CA080946

References

1. Davis CD, Irons R. Are selenoproteins important for the cancer protective effects of selenium? Curr Nutrition & Food Sci 2005;1:201–214.
2. Clark LC, Combs GF Jr, Turbull BW, et al. Effects of selenium supplementation for cancer prevention in patients with carcinoma of the skin. A randomized control trial Nutritional Prevention of Cancer Study Group. JAMA 1996;276:1957–63. [PubMed: 8971064]

3. Davis CD, Uthus EO. Dietary folate and selenium affect dimethylhydrazine-induced aberrant crypt formation, global DNA methylation and one-carbon metabolism in rats. J Nutr 2003;133:2907–14. [PubMed: 12949386]
4. Jao SW, Shen KL, Lee W, Ho YS. Effect of selenium on 1,2-dimethylhydrazine-induced intestinal cancer in rats. Dis Colon Rectum 1996;39:628–31. [PubMed: 8646947]
5. Irons R, Carlson BA, Hatfield DL, Davis CD. Both selenoproteins and low molecular weight selenocompounds reduce colon cancer risk in mice with genetically impaired selenoprotein expression. J Nutr 2006;135:1311–1317. [PubMed: 16614422]
6. Kryukov GV, Castellano S, Novoselov SV, et al. Characterization of mammalian selenoproteomes. Science 2003;300:1439–43. [PubMed: 12775843]
7. Kumaraswamy E, Malykjh A, Korotkov KV, et al. Structure-expression relationships of the 15-kDa selenoprotein gene. J Biol Chem 2000;275:35540–35547. [PubMed: 10945981]
8. Labusky VM, Hatfield DL, Gladyshev VN. The Sep15 protein family: roles in disulfide bond formation and quality control in the endoplasmic reticulum. 2007;59:1–5.
9. Nasr MA, Hu YJ, Diamond AM. Allelic loss of the Sep15 locus in breast cancer. Cancer Ther 2004;1:293–298.
10. Corbett TH, Girswold DP Jr, Roberts BJ, Peckham JC, Schabel FM Jr. A mouse colon-tumor model for experimental therapy. Cancer Chemother Rep 1975;5:169–186.
11. Yoo MH, Xu XM, Carlson BA, Gladyshev VN, Hatfield DL. Thioredoxin reductase 1 deficiency reverses tumor phenotypes and tumorigenicity of lung carcinoma cells. J Biol Chem 2006;281:13005–13008. [PubMed: 16565519]
12. Xu XM, Mix H, Carlson BA, Grabowski PJ, Gladyshev VN, Berry MJ, Hatfield DL. Evidence for direct roles of two additional factors, SECp43 and soluble liver antigen, in the selenoprotein synthesis machinery. J Biol Chem 2005;280:41568–41575. [PubMed: 16230358]
13. Carlson BA, Xu XM, Gladyshev VN, Hatfield DL. Selective rescue of selenoprotein expression in mice lacking a highly specialized methyl group in selenocystein tRNA. J Biol Chem 2005;280:5542–5548. [PubMed: 15611090]
14. Paglia DE, Valentine WN. Studies on the quantitative and qualitative characterization of erythrocyte glutathione peroxidase. J Lab Clin Med 1967;70:158–69. [PubMed: 6066618]
15. Holmgren A, Bjornstedt M. Thioredoxin and thioredoxin reductase. Methods Enzymol 1995;252:199–208. [PubMed: 7476354]
16. Hill KE, McCollum GW, Burk RF. Determination of thioredoxin reductase activity in rat liver supernatant. Anal Biochem 1997;253:123–5. [PubMed: 9356150]
17. Hintze KJ, Wald KA, Zeng H, Jeffery EH, Finley JW. Thioredoxin reductase in human hepatoma cells is transcriptionally regulated by sulforaphane and other electrophiles via an antioxidant response element. J Nutr 2003;133:2721–7. [PubMed: 12949356]
18. Huang DW, Sherman BT, Lempicki RA. Systematic and integrative analysis of large gene lists using DAVID Bioinformatics Resources. Nature Protoc 2009;4:44–57. [PubMed: 19131956]
19. Dennis G Jr, Sherman BT, Hosack DA, Yang J, Gao W, Lane HC, Lempicki RA. DAVID: Database for Annotation, Visualization, and Integrated Discovery. Genome Biol 2003;4:P3. [PubMed: 12734009]
20. Apostolou S, Klein JO, Missuuchi Y, et al. Growth inhibition and induction of apoptosis in mesotheliuma cells by selenium and dependence on selenoprotein *SEP15* genotype. Oncogene 2004;23:5032–5040. [PubMed: 15107826]
21. Jablonska E, Gromadzinska J, Sobala W, Reszka E, Wasowicz W. Lung cancer risk associated with selenium status is modified in smoking individuals by *Sep15* polymorphism. Eur J Cancer 2008;47:47–54.
22. Yoo MH, Xu YM, Carlson BA, Patterson AD, Gladyshev VN, Hatfield DL. Targeting thioredoxin reductase 1 reduction in cancer cells inhibits self-sufficient growth and DNA replication. PLOS One 2007;2:e1112. [PubMed: 17971875]
23. Arner ES, Holmgren A. Physiological functions of thioredoxin and thioredoxin reductase. Eur J Biochem 2000;267:6102–6109. [PubMed: 11012661]
24. Labusky VY, Hatfield DL, Gladyshev VM. The Sep 15 protein family: roles in disulfide bond formation and quality control in the endoplasmic reticulum. Life 2007;59:1–5. [PubMed: 17365173]

25. Hanahan D, Weignerg RA. The hallmarks of cancer. Cell 2000;100:50–70.

26. Toby GG, Gherraby W, Coleman TR, Golemis EA. A novel RING finger protein, human enhancer of invasion 10, alters mitotic progression through regulation of cyclin B levels. Mol Cell Biol 2003;23:2109–2122. [PubMed: 12612082]

27. Singh MK, Nicolas E, Gherraby W, Dadke D, Lessin S, Golemis EA. He110 negatively regulates cell invasion by inhibiting cyclin B/cdk1 and other promotility proteins. Oncogene 2007;26:4825–4832. [PubMed: 17297447]

28. Confalonieri S, Quarto M, Goisis G, Nuciforo P, Donzelli M, Jodice G, Peolis G, Viale G, Pece S, diFiore PP. Alteration of ubiquitin ligases in human cancer and their association with the natural history of the tumor. Oncogene 2009;28:2959–2968. [PubMed: 19543318]

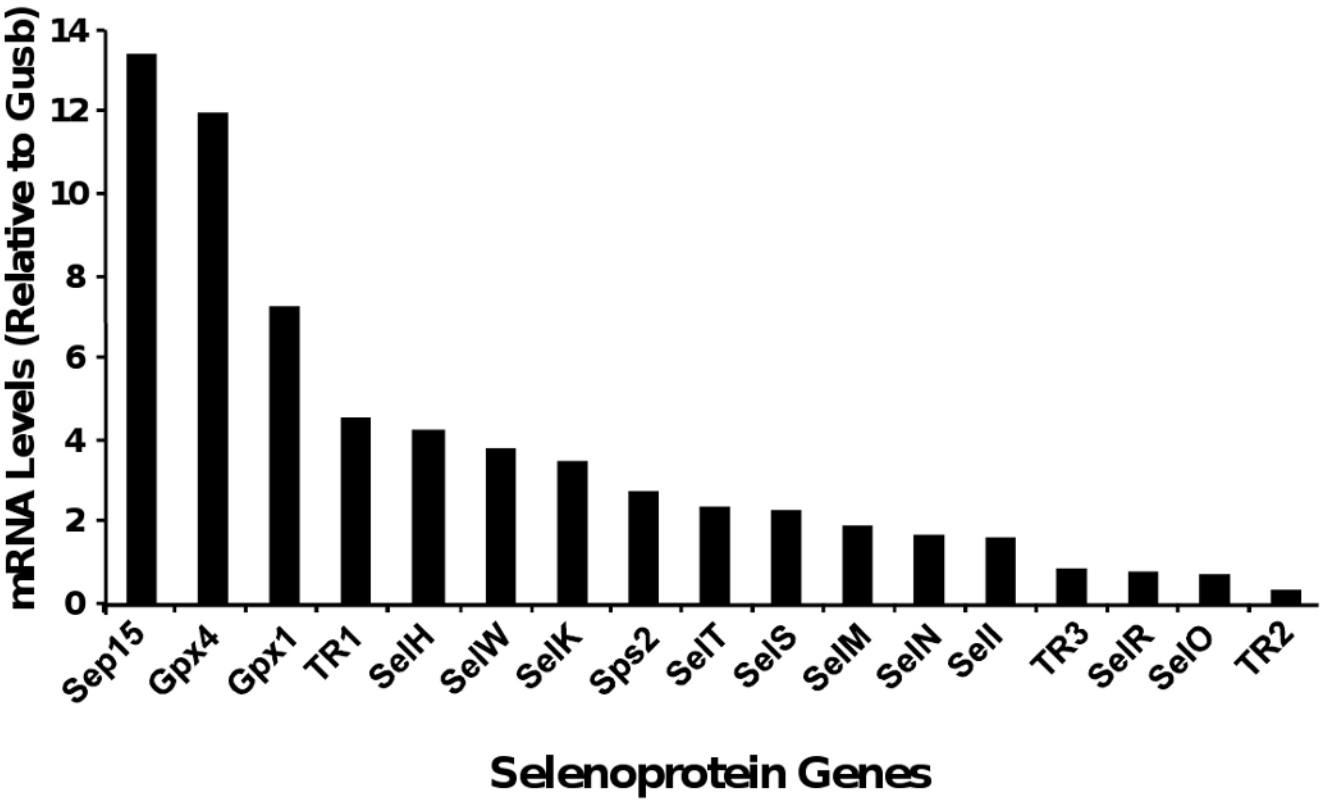

Figure 1.
Selenoprotein mRNA expression in CT26 cells. Cells were grown, RNA extracted and mRNA levels for indicated selenoproteins determined by RT-PCR analysis as described in Materials and Methods. β-Glucuronidase (*Gusb*) was utilized as the internal control.

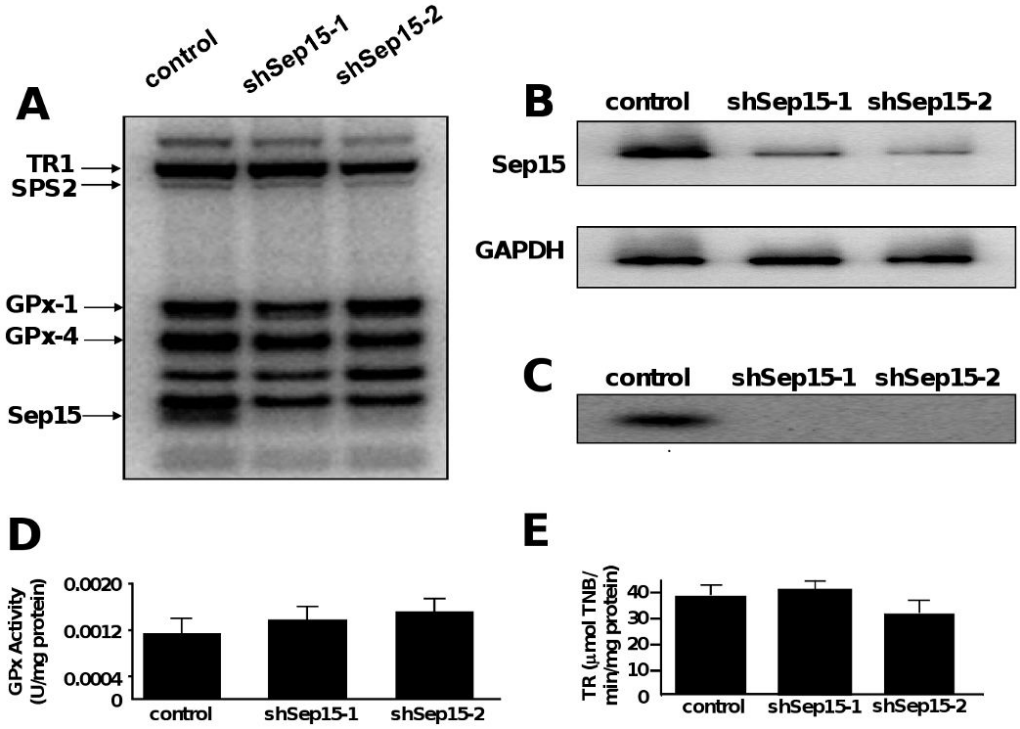

Figure 2.

Targeted removal of Sep15 in CT26 cells. Cells were stably transfected with the pU6-m3 control, shSep15-1 or shSep15-2 construct (as indicated) and the expression of Sep15 examined by labeling cells with ^{75}Se (A), northern blotting (B) or western blotting (C). Transfected cells were also analyzed for glutathione peroxidase (D) and thioredoxin reductase (E) activities. Values are mean ± SEM (n=3)

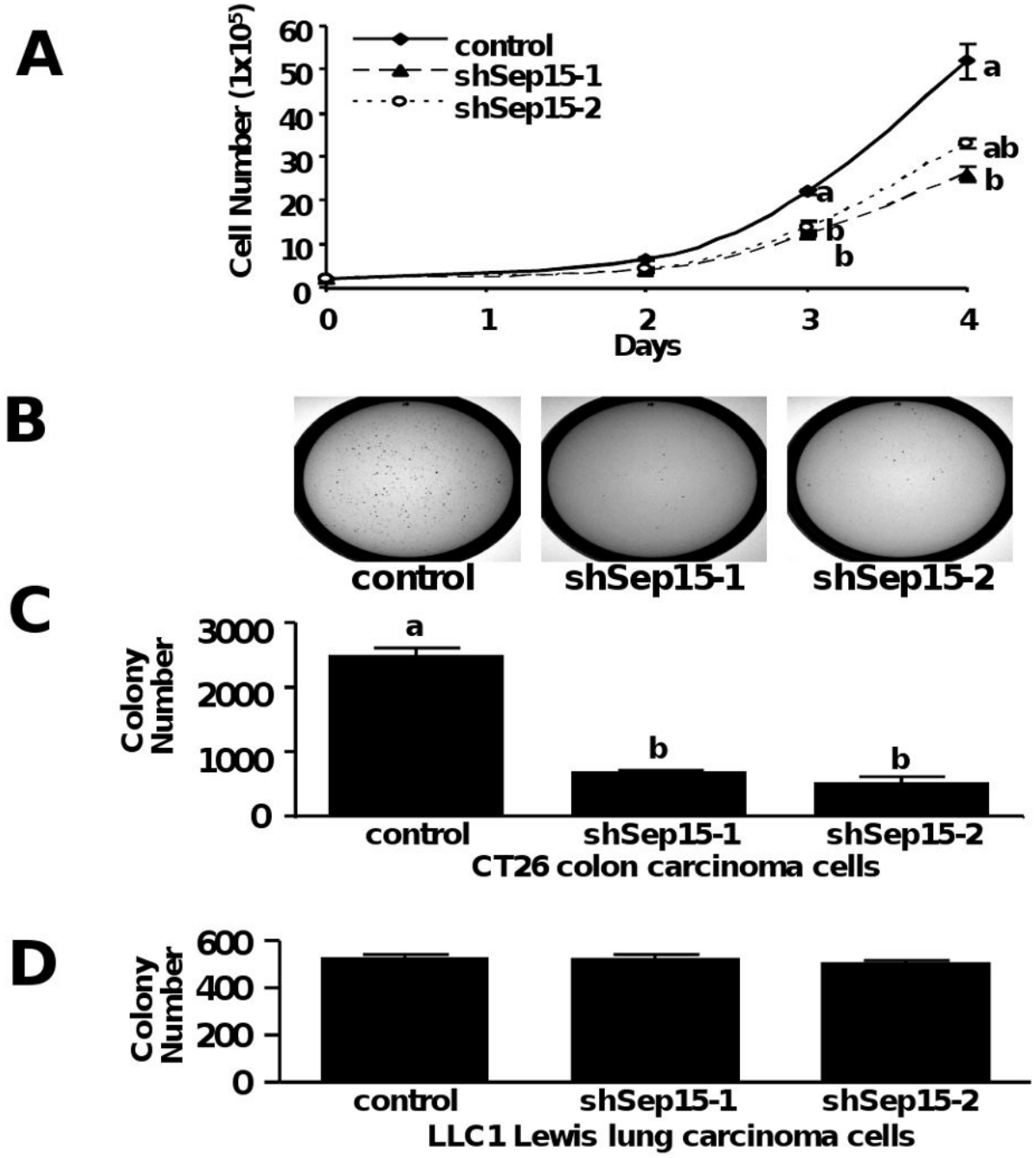

Figure 3.

Effects of targeted down-regulation of Sep15 on cell growth and colony formation in soft agar in CT26 cells and LLC1 cells. Growth rates of cells transfected with the pU6-m3 control, shSep15-1 or shSep15-2 construct (A). Ability of cells transfected with the pU6-m3 control, shSep15-1 or shSep 15-2 constructs to grow in soft agar. CT26 colonies were stained with *p*-iodonitrotetrazolium overnight (B) and the stained colonies were counted and recorded (C). The ability of LLC1 cells transfected with the control, shSep15-1 and shSep15-2 constructs to grow in soft agar were assessed and quantitated (D). Values are mean ±SEM, n=3 for CT26 cells and n=8 for LLC1 cells. Data are indicative of 3 independent experiments. Means not sharing a common letter are significantly different, $p < 0.01$.

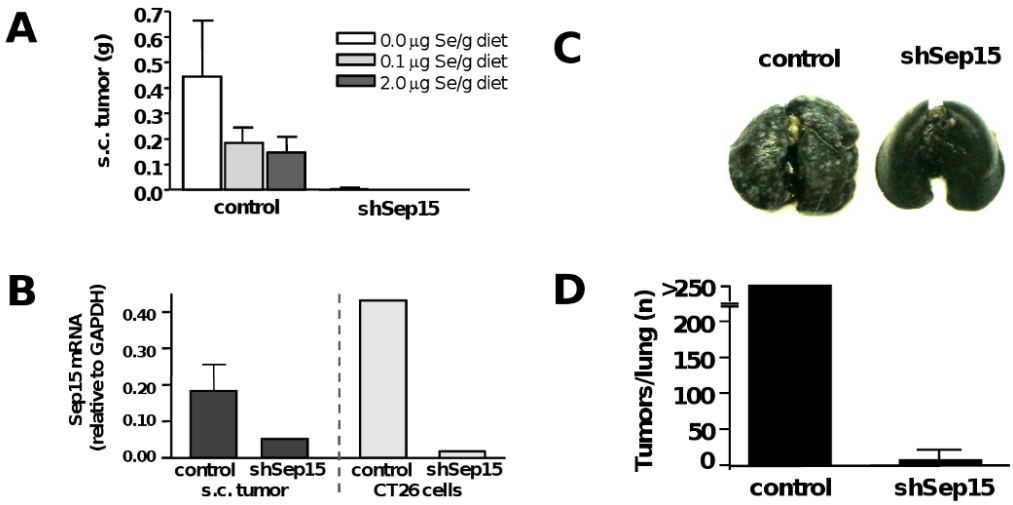

Figure 4.

Effects of targeted down-regulation of Sep15 on primary tumor formation and lung metastases in BALB/c mice. Mice maintained on Se-deficient (0 μg S/g), Se-sufficient (0.1 μg S/g), and Se-enriched (2 μg S/g) diets were injected subcutaneously with 1×10^6 control or shSep15 CT26 cells and after three weeks, mice were sacrificed, tumors excised and weighed (A). qRT-PCR analysis of Sep15 mRNA from tumor samples from mice injected with control or cells with targeted down-regulation ofSep15 and mRNA from the cells (B). Mice were injected i.v. with 5×10^5 pU6-m3 control or shSep15 cells. Twelve days after injection, lungs were excised and "bleached" by Fekete's solution. Lung metastases appear white (C). Lesions formed on the surface of each lung were counted; lungs with more than 250 metastatic lesions were assigned a value of 250 (D). Values are means ± SEM (n=4). Data are indicative of 3 independent experiments. Means not sharing a common letter are significantly different, $p< 0.0001$.

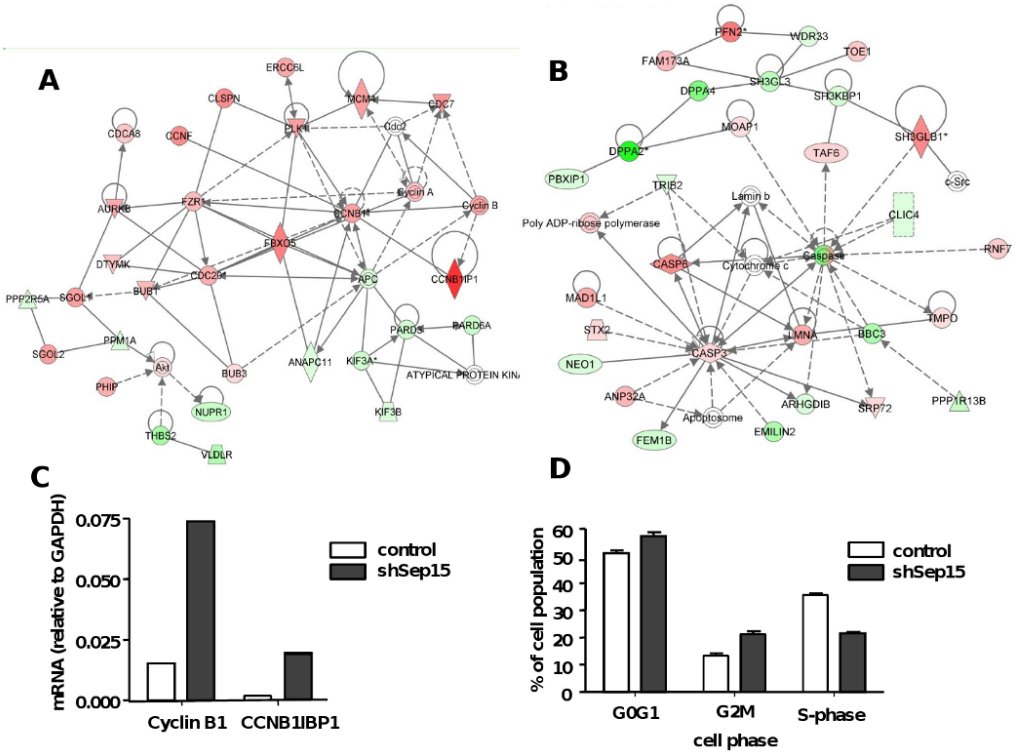

Figure 5.

Ingenuity network analysis of genes regulated by targeted down-regulation of Sep15 in CT26 cells and validation by qRT-PCR and cell cycle analysis. Two of the top associated networks were: cell cycle/cancer (A) and cancer/cell-to-cell signaling and interaction/cellular function and maintenance (B). Probe sets identified as differentially expressed were imported into Ingenuity Pathway Analysis software. Pink indicates an upregulation and green a downregulation of gene expression. Molecules that are not user specified, but are incorporated into the network through relationships with other molecules, are shown in white. qRT-PCR analysis of cyclin B and CCNB1IP1 mRNA expression in control and cells with targeted down-regulation (C). Percent of cells in each phase of the cell cycle as determined by FACS analysis (D). Values are mean ± SEM, n=8.

Table 1

Genes and protein products whose expression was regulated by knockdown of Sep15 in CT26 colon cancer cells.

Gene change	Product	fold
Upregulated in shSep15 CT26 cells:		
Ccnb1ip1	cyclin B1 interacting protein 1	13.52
Myoz2	myozenin 2	9.36
Elovl6	ELOVL family member 6, elongation of long chain fatty acids	8.55
Atp8a1	ATPase, aminophospholipid transporter (APLT)	7.69
Tyw3	tRNA-yW synthesizing protein 3 homolog	7.54
Aqp1	aquaporin 1 (Colton blood group)	6.33
Serpine1	serpin peptidase inhibitor, clade E	6.03
Spint2	serine peptidase inhibitor, Kunitz type, 2	5.83
Acadm	acyl-Coenzyme A dehydrogenase	5.70
Dscc1	defective in sister chromatid cohesion 1 homolog	5.52
Sfmbt2	Scm-like with four mbt domains 2	5.42
Kcnab2	potassium voltage-gated channel, shaker-related subfamily	5.35
Tuba4a	tubulin, alpha 4a	5.34
Tcf19	transcription factor 19	5.30
Chtf18	CTF18, chromosome transmission fidelity factor 18 homolog	5.12
Ccne2	cyclin E2	4.70
Downregulated in shSep15 CT26 cells		
Lrrn4cl	LRRN4 C-terminal like	0.02
Afp	alpha-fetoprotein	0.02
Mamdc2	MAM domain containing 2	0.02
Dppa2	developmental pluripotency associated 2	0.03
Arhgef5	Rho guanine nucleotide exchange factor (GEF) 5	0.03
Nefl	neurofilament, light polypeptide	0.03
Avil	advillin	0.03
Klf2	Kruppel-like factor 2 (lung)	0.05
Atp1a3	ATPase, Na+/K+ transporting, alpha 3 polypeptide	0.07
Slit3	slit homolog 3 (Drosophila)	0.07
Ifitm1	interferon induced transmembrane protein 1 (9-27)	0.08
Odz4	odz, odd Oz/ten-m homolog 4 (Drosophila)	0.08
Pla2g2e	phospholipase A2, group IIE	0.08
Igfbp4	insulin-like growth factor binding protein 4	0.08
Rab33a	RAB33A, member RAS oncogene family	0.09
Grem1	gremlin 1, cysteine knot superfamily	0.09
Prss12	protease, serine, 12 (neurotrypsin, motopsin)	0.09
Stard5	StAR-related lipid transfer (START) domain containing 5	0.10
Pdgfrb	platelet-derived growth factor receptor, beta polypeptide	0.10
Napb	N-ethylmaleimide-sensitive factor attachment protein, beta	0.11
Casp4	caspase 4, apoptosis-related cysteine peptidase	0.11